Inorganic Chemistry

ARTICLE

pubs.acs.org/IC

Inducing Effect of Additive Agents on Coordination Assembly of Silver(I) Nitrate with 3,5-Bis(2-pyridyl)-4-amino-1,2,4-triazole: Supramolecular Isomerism and Interconversion

Cheng-Peng Li,[†] Jing-Min Wu,[†] and Miao Du*[,†,‡]

[†]College of Chemistry, Tianjin Key Laboratory of Structure and Performance for Functional Molecule, Tianjin Normal University, Tianjin 300387, P. R. China

[‡]State Key Laboratory of Structural Chemistry, Fujian Institute of Research on the Structure of Matter, Chinese Academy of Sciences, Fuzhou, Fujian 350002, P. R. China

Supporting Information

ABSTRACT: By using different organic acids as additive agents, hydrothermal reactions of $AgNO_3$ with 3,5-bis(2-pyridyl)-4-amino-1,2,4-triazole (2-bpt) lead to formation of two conformational polymorphs of $[Ag(2\text{-bpt})](NO_3)$ with bimetallocyclic and 1-D helical coordination patterns. Interconversion between the two supramolecular isomers can be achieved under proper conditions, which will pass through the same intermediate state.

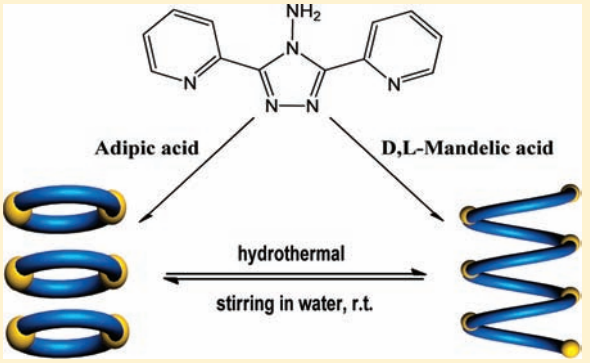

INTRODUCTION

Supramolecular isomerism (or polymorphism), in one sense a complication, is of great importance in several areas such as organic crystals, inorganic materials, and hybrid metal−organic frameworks.[1] Study of supramolecular isomers may allow one to obtain a better understanding of the factors influencing the crystal growth and formation of novel crystalline materials.[2] In this connection, the most important challenge is to control generation of particular superstructures for imaginable supramolecular isomers with the same composition. At present, it has been well demonstrated that the intrinsic diversity of ligand function (binding fashion, conformation, orientation, etc.) and some external factors (such as solvent and temperature used for crystallization) may result in supramolecular isomerism of coordination assemblies.[3−5] For example, Lu et al. recently reported a series of supramolecular isomers constructed from *cis*-$[Ni(f\text{-}rac\text{-}L)]^{2+}$ (L = 5,5,7,12,12,14-hexamethyl-1,4,8,11-tetraazacyclotetradecane) and $[Ni(CN)_4]^{2-}$ building blocks, which are quite sensitive to the experimental conditions.[3c,d] Moreover, one achiral and four homochiral supramolecular isomers can be obtained from the same reaction system of the racemic $[Ni(rac\text{-}L)]^{2+}$ tecton and $[Fe(CN)_5NO]^{2-}$.[3e] Undoubtedly, such phenomena indicate the considerable difficulty in predicting the crystal structure of a specific coordination assembly. Additionally, reports on the solid-state conversions between supramolecular isomers are of further interest but quite scarce so far.[6] In this regard, it has recently been known that structural rearrangement of coordination assemblies may occur in the solid state, in response to external physical and/or chemical stimuli through thermodynamic and kinetic control, where single-crystal to single-crystal transformation is of special fascination.[7,8] Significantly, in some cases, such dynamic processes are concomitant with the dramatic changes of crystal structures and may facilitate formation of distinct supramolecular isomers.

Recently, we designed and constructed a variety of coordination supramolecular systems with the angular dipyridyl ligand bis(4-pyridyl)-4-amino-1,2,4-triazole (4-bpt) and its 3-pyridyl analog (3-bpt).[9] In this context, as an extension of our research, we report herein the supramolecular isomerism and structural conversion observed in the coordination assembly of 3,5-bis-(2-pyridyl)-4-amino-1,2,4-triazole (2-bpt) with silver(I) nitrate. Reaction of 2-bpt and $AgNO_3$ under hydrothermal conditions in the presence of different organic acids as additive agents yields two supramolecular isomers $[Ag(2\text{-bpt})]_2(NO_3)_2$ (**1**) and $\{[Ag(2\text{-bpt})](NO_3)\}_n$ (**2**) with dinuclear and 1-D helical coordination motifs, respectively. Furthermore, structural transformations between the two isomeric phases, which interestingly undergo the same intermediate state, have also been determined and discussed in detail.

Received: March 16, 2011
Published: September 08, 2011

Table 1. Crystal Data and Structural Refinement Summary for Complexes 1 and 2

	1	2
chemical formula	$C_{24}H_{20}Ag_2N_{14}O_6$	$C_{12}H_{10}AgN_7O_3$
fw	816.28	408.14
cryst size (mm)	0.28 × 0.22 × 0.20	0.38 × 0.36× 0.30
cryst syst	monoclinic	orthorhombic
space group	$P2_1/c$	$P2_12_12_1$
a (Å)	8.5415(5)	7.4816(6)
b (Å)	24.4718(13)	8.1746(7)
c (Å)	6.9908(4)	22.8228(18)
β (deg)	109.9960(10)	90.00
V (Å^3)	1373.17(13)	1395.8(2)
Z	2	4
ρ_{calcd} (g cm^{-3})	1.974	1.942
μ (mm^{-1})	1.479	1.473
F(000)	808	808
total/independent reflns	2427/2075	2466/2390
parameters	208	208
R_{int}	0.0182	0.0151
R,[a] R_w[b]	0.0297, 0.0700	0.0228, 0.0574
GOF[c]	1.042	1.081

[a] $R = \Sigma||F_o| - |F_c||/\Sigma|F_o|$. [b] $R_w = [\Sigma[w(F_o^2 - F_c^2)^2]/\Sigma w(F_o^2)^2]^{1/2}$. [c] GOF = $\{\Sigma[w(F_o^2 - F_c^2)^2]/(n-p)\}^{1/2}$.

EXPERIMENTAL SECTION

Materials and General Methods. With the exception of the ligand 2-bpt that was synthesized according to the literature procedure,[10] all of the starting reagents and solvents were obtained commercially and used as received without further purification. Fourier transform (FT) IR spectra (with KBr pellets) were taken on an AVATAR-370 (Nicolet) spectrometer. Elemental analyses of carbon, hydrogen, and nitrogen were performed on a CE-440 (Leemanlabs) analyzer. Powder X-ray diffraction (PXRD) patterns were recorded on a Shimadzu Maxima XRD-7000 diffractometer at 30 kV and 100 mA for a Cu-target tube (λ = 1.5406 Å), with a scan speed of 2°/min and a step size of 0.02° in 2θ. The calculated PXRD patterns were simulated from the single-crystal X-ray diffraction data by using the PLATON program. Thermogravimetric (TG) and differential scanning calorimetric (DSC) analysis experiments were carried out on a NETZSCH TG 209 thermal analyzer from 25 to 800 °C under N_2 atmosphere at a heating rate of 10 °C/min. The solid-state fluorescence spectra were obtained by using a Cary Eclipse (Varian) spectrofluorimeter at room temperature. Solid-state circular dichroism (CD) spectra (with KBr pellets) were recorded on a Jasco J-810 spectropolarimeter.

Synthesis of 1 and 2. *[Ag(2-bpt)]$_2$(NO$_3$)$_2$ (**1**).* A mixture of 2-bpt (23.8 mg, 0.1 mmol), $AgNO_3$ (17.0 mg, 0.1 mmol), and adipic acid (14.6 mg, 0.1 mmol) in H_2O (15 mL) was sealed in a Teflon-lined stainless steel vessel (20 mL), which was heated at 100 °C for 3 days and then cooled to room temperature for 1 day at a rate of 5 °C/h. Colorless block crystals of **1** were collected in 58% yield (23.6 mg). Anal. Calcd for $C_{24}H_{20}Ag_2N_{14}O_6$ (**1**): C, 35.32; H, 2.47; N, 24.02. Found: C, 35.27; H, 2.63; N, 24.11. IR (cm^{-1}): 3330m, 1595s, 1513w, 1487w, 1465s, 1424s, 1382vs, 1313vs, 1286vs, 1159m, 1099w, 1067w, 1043w, 997m, 894w, 793s, 742s, 699m, 626w, 498w.

*{[Ag(2-bpt)](NO$_3$)}$_n$ (**2**).* Colorless block crystals of **2** were obtained in 56% yield (23.0 mg) using the same synthetic procedure as that for **1**, except that adipic acid was replaced by D,L-mandelic acid (15.2 mg, 0.1 mmol). Anal. Calcd for $C_{12}H_{10}AgN_7O_3$ (**2**): C, 35.32; H, 2.47; N, 24.02. Found: C, 35.43; H, 2.54; N, 24.08. IR (cm^{-1}): 3273m, 1592s, 1570w, 1491w, 1463s, 1385vs, 1314s, 1278m, 1154w, 1070w, 1036w, 999m, 796s, 742m, 698s, 629w, 525w.

Single-Crystal X-ray Diffraction. Single-crystal X-ray diffraction data for **1** and **2** were collected on a Bruker Apex II CCD diffractometer with Mo Kα radiation (λ = 0.71073 Å) at room temperature. Semi-empirical absorption corrections were applied using the SADABS program, and the program SAINT was used for integration of the diffraction profiles.[11] The structures were solved by direct methods using the SHELXS program of the SHELXTL package and refined with SHELXL.[12] The final refinements were performed by full-matrix least-squares methods on F^2 with anisotropic thermal parameters for all non-H atoms. Generally, C-bound hydrogen atoms were placed geometrically and refined as riding, whereas N-bound H atoms were first determined in difference Fourier maps and then fixed in the calculated positions. Isotropic displacement parameters of the H atoms were derived from their parent atoms. Further crystallographic details are listed in Table 1, and selected bond parameters are shown in Table S1 (Supporting Information).

RESULTS AND DISCUSSION

General Synthesis and Characterization. In this work, complexes **1** and **2** were similarly prepared under hydrothermal conditions by adding different additive agents adipic acid (for **1**) and D,L-mandelic acid (for **2**). In each case, the crystalline product was fully characterized by IR, elemental analysis, and single-crystal X-ray diffraction techniques, and the phase purity of the bulk sample was further confirmed by the PXRD pattern (see Figure S1a and S1b, Supporting Information). In the IR spectra of **1** and **2**, the characteristic absorption peaks of the nitrate anions appear at 1382 and 1385 cm^{-1}, respectively.

Notably, under the same synthetic conditions of **1** and **2**, reaction of 2-bpt and $AgNO_3$ without any additive agent only results in a clear pale-yellow solution, that is, no solid-state product could be directly obtained after the reaction vessel was cooled to room temperature for 1 day, which reveals the critical role of additive agents in the crystallization of **1** and **2**. However, white floccules will be observed when this pale-yellow solution is placed in the dark for over 1 week upon solvent evaporation, and this product is confirmed to be complex **1** according to a comparison of their PXRD patterns (see Figure S1c, Supporting Information), that is, additive agent is not necessary in formation of **1**, which however can significantly promote crystal growth in a shorter course.

*Crystal Structure of [Ag(2-bpt)]$_2$(NO$_3$)$_2$ (**1**).* Single-crystal X-ray diffraction results indicate that the asymmetric unit of complex **1** is composed of one Ag^I ion, one 2-bpt ligand, and one NO_3^- counterion. Each ligand is chelated to a pair of Ag^I ions via the pyridyl−triazole segments. Each Ag^I center adopts the distorted square planar geometry, provided by four nitrogen donors from two 2-bpt ligands with the Ag−N lengths in the range of 2.300(3)−2.435(3) Å (see Table S1, Supporting Information, for details). As a result, a pair of Ag^I centers are combined by two 2-bpt ligands to produce a [2 + 2] dimeric metallacycle (see Figure 1a) with centrosymmetry, where the intramolecular Ag···Ag separation is 4.829(1) Å. The two 2-pyridyl rings in each 2-bpt ligand, with a dihedral angle of 3.6°, adopt the *cis* conformation and are away from the 4-amino group to meet the coordination requirement, which deviate from the central triazole group with dihedral angles of 21.1° and 20.5°. Additionally, there exist N5−H5A···O3 (H···O/N···O = 2.38/3.066 Å

dx.doi.org/10.1021/ic200540c |*Inorg. Chem.* 2011, 50, 9284–9289

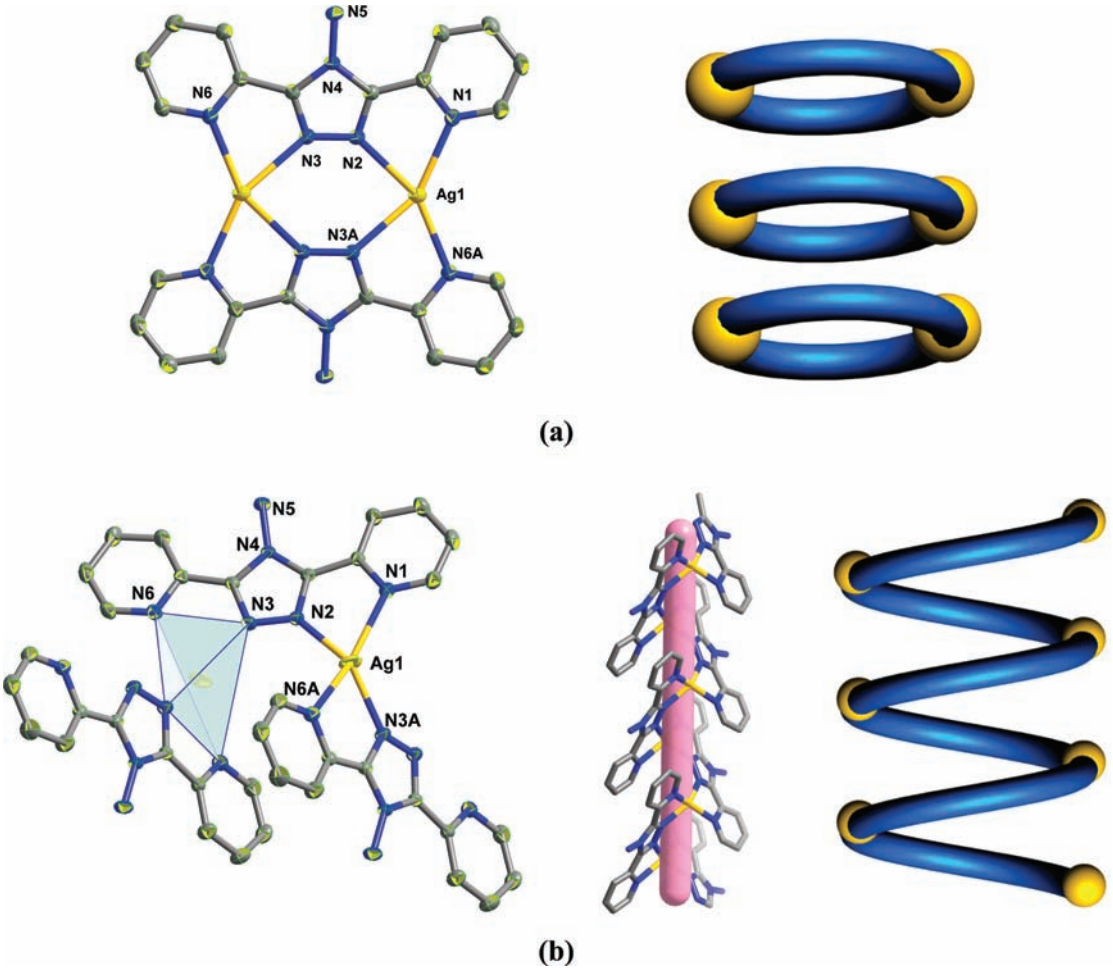

Figure 1. Views of the supramolecular isomers for (a) the dinuclear motif in **1** and (b) the 1-D helical chain in **2**. Symmetry codes: A = $-x + 1, -y + 2, -z + 1$ for **1**; A = $x - 1/2, -y + 3/2, -z$ for **2**.

and N−H···O = 134°) and N5−H5B···O2^{i} (H···O/N···O = 2.11/2.957 Å and N−H···O = 158°; $i = x, y, z - 1$) H-bonding interactions between the amino groups of 2-bpt and the nitrate anions, which connect such dinuclear motifs to afford a 1-D ladder-like chain (see Figure S2, Supporting Information).

Crystal Structure of $\{[Ag(2\text{-bpt})](NO_3)\}_n$ (**2**). Isolation of **1** reveals that the crystalline product may be finely induced by a particular organic acid as the additive agent. Therefore, we also explored the role of other additive agents in such an assembled system (see the following discussion for details). As a result, a 1-D chiral helical species **2** is formed with the aid of D,L-mandelic acid as a supramolecular isomer of **1**. In the crystal structure of **2**, the coordination environment of Ag^{I} and the binding mode of the 2-bpt ligand are similar to those observed in **1** (see Figure 1b). Notably, the four-coordinated geometry of Ag^{I} is more distorted in this case with the Ag−N lengths of 2.222(2)−2.507(3) Å (see Table S1, Supporting Information, for details), while the planarity of 2-bpt is evidently improved, that is, the dihedral angle between the two 2-pyridyl groups is 1.3°, which deviate from the central triazole ring of 9.6° and 10.7°. In this way, the 2-bpt ligands link the Ag^{I} ions to form an infinite 1-D array that winds around the crystallographic 2_1 axis, with an adjacent Ag···Ag distance of 4.300(1) Å. The pitch of each right-handed helix is 7.4816(6) Å, which is equal to the length of the *a* axis. Similarly, the lattice nitrate anions are also H-bonded to the amino groups of 2-bpt via N5−H5A···O2 (H···O/O···N = 2.15/2.990 Å and N−H···O = 167°) and N5−H5B···O2^{i} (H···O/O···N = 2.15/2.977 Å and N−H···O = 165°; $i = -x + 1, y + 1/2, -z + 1/2$) interactions, affording a 3-D supramolecular architecture (see Figure S3, Supporting Information). Significantly, all 1-D helices thereof possess the same

Scheme 1. Possible Additive Agents for Preparation of 1

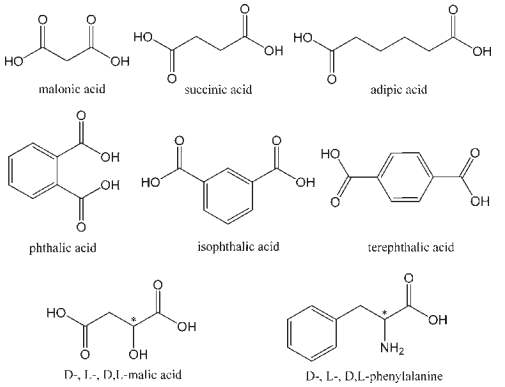

dx.doi.org/10.1021/ic200540c |*Inorg. Chem.* 2011, 50, 9284–9289

Scheme 2. Possible Synthetic Methods for 1 and 2

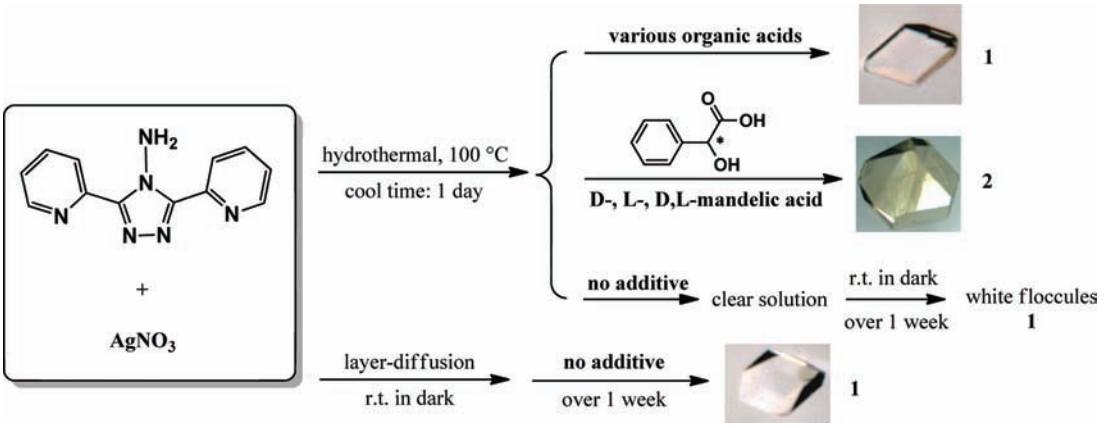

handedness, which thus results in the homochiral nature of **2** with a flack parameter of 0.02(3).

Role of Additive Agents in Coordination Assemblies. Our initial experiments reveal that the additive agents (different organic acids) are critical to form supramolecular isomers **1** and **2**. In order to adequately explore the role of additive agents and other factors on the assembled system of silver(I) and 2-bpt, we carried out a series of related experiments. On the one hand, complex **1** can also be prepared under similar conditions using a variety of organic acids as additives, such as aliphatic acids, benzenedicarboxylic acids, and even chiral acids comparable to mandelic acid used in **2** (see Scheme 1). However, formation of the chiral helical complex **2** shows a specificity to the additive of D-, L-, or D,L-mandelic acid, at least for the current experimental results. On the other hand, the dinuclear species **1** can be obtained from the same starting materials ($AgNO_3$, 2-bpt, and adipic acid) under various conditions via changing the reaction temperature, solvent, and stoichiometric ratio of reactants (see Table S2, Supporting Information, for detailed parameters). However, no crystalline solid will be formed if the reaction conditions of **2** are similarly changed. In addition, complex **1** can also be isolated by evaporating the hydrothermal reaction solution without any additive agent for a long time (over 1 week, vide supra) or using the layer-diffusion method of water ($AgNO_3$) and methanol (2-bpt) solutions at ambient conditions over 1 week. The above results clearly indicate that complex **1** is statistically found to be the more universal and favorable product compared with **2** for such a coordination assembly (see Scheme 2). According to the viewpoint of transition state theory, specific supramolecular isomers should be the most favorable species under different reaction conditions. Herein, complex **1** may be regarded as the thermodynamic isomer for such a system, which is also supported by the experimental results of structural transformations between **1** and **2** as discussed below.

Another appealing issue is the origin of the chiral nature of isomer **2**. Construction of a chiral metallosupramolecular assembly using the achiral ligand may be achieved by chiral induction, that is, to induce chirality of the crystalline product through an external force, usually chemical in nature.[13] As a rule, such a chiral induction can be accomplished by virtue of chiral solvent (organic solvent and ionic liquid)[14] or chiral additive agent,[15] which may arouse particular weak interactions, such as solvent–solvate contacts, van der Waals forces, hydrogen bonds, and $\pi\cdots\pi$ stacking. In fact, the chiral sites in the additive agents and the associated intermolecular interactions between the chiral additive and the achiral tecton can be sufficient to direct the homochirality in a particular crystallization process.[15] In the case of **2**, D,L-mandelic acid can be considered as the chiral additive, and in order to further understand its intrinsic role in inducing the crystallization, the solid-state CD spectra (see Figure S4, Supporting Information) of **2** were measured. Obviously, the bulk samples of **2**, which are prepared in the presence of enantiopure D- or L-mandelic acid and racemic D,L-mandelic acid, respectively, are CD silent in all cases. This result reveals that the crystalline products of **2** will be racemic (spontaneous resolution) and independent of the chirality of mandelic acid additive.

In fact, the isomerism arising from the additive effect is accidentally observed since the additive is not included in the final crystalline product. Though more theoretical and experimental efforts are required to demonstrate the role of additive agents in inducing the different supramolecular isomers, some general rules may be assumed at this stage. Normally the additives have strong binding capability, large size, and low concentration in the reaction system and thus may impact the solvation process and coordination kinetics in solution.[15b] Comparing the additive agents used in formation of complexes **1** and **2**, we conclude that the familiar achiral aliphatic and aromatic acids will promote crystal growth of **1**. However, it should be noted that the chiral additive agents malic acid and phenylalanine used for preparing **1** are structurally similar to mandelic acid used for preparing **2**, demonstrating their high selectivity and sensitivity in such a coordination assembly. Accordingly, it can be temporarily deduced that the synergistic effect of the chiral center, stereochemistry (presence of phenyl), and potential interacting sites for H-bonding (hydroxyl) and aromatic stacking (phenyl) of mandelic acid may direct the crystallization of **2**, while the other additive agents will play a completely different role and be responsible for production of its supramolecular isomer **1**, although all of them are not included in the resulting crystals.

Transformations between 1 and 2. Both isomers **1** and **2** are insoluble in water. The single crystals of **2** will lose the single crystallinity under stirring in water and gradually transform to white powders after several hours. Remarkably, the time-resolved PXRD patterns (see Figure 2a) show that a new species **3** is formed after ca. 16 h, which however will be completely

dx.doi.org/10.1021/ic200540c |*Inorg. Chem.* 2011, 50, 9284–9289

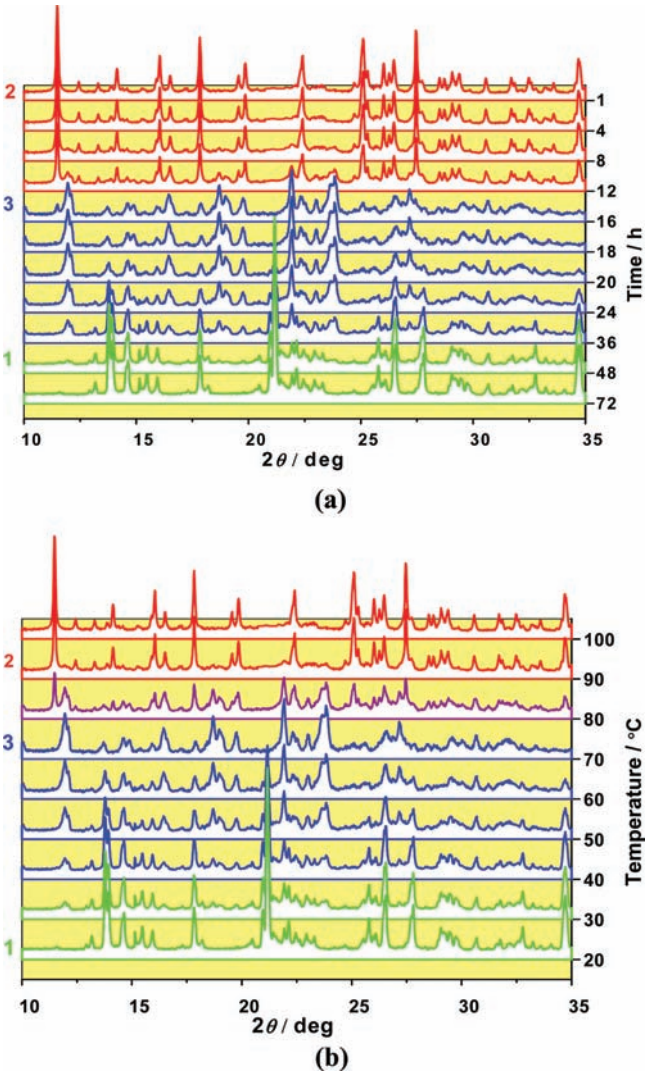

Figure 2. (a) Time-resolved PXRD patterns for the structural transformation from **2** to **1**. (b) Temperature-resolved PXRD patterns for structural transformation from **1** to **2**.

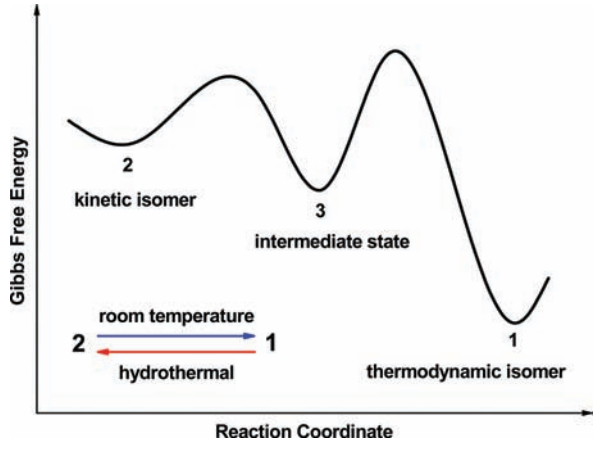

Figure 3. Proposed reaction coordinate diagram demonstrating the interconversion between supramolecular isomers **1** (thermodynamic) and **2** (kinetic).

transformed to isomer **1** after stirring for ca. 2 days. Though the crystal structure of **3** cannot be properly determined after many tries, we conclude that **3** is different than **1** and **2** according to comparisons of their elemental analyses (found for **3**: C, 39.66; N, 16.14; H, 2.85), PXRD patterns (see Figure S5, Supporting Information), IR spectra (see Figure S6, Supporting Information), and TG-DSC curves (see Figure S7, Supporting Information). Notably, if single crystals of **2** are exposed to air in the solid state, a color change from colorless to gray will be observed after 2 days. However, no structural transformation occurs in this course, as confirmed by PXRD patterns. This result indicates that the above transformation from **2** to **1** should be a solvent-mediated process.

Moreover, an inverse structural conversion can also be achieved,[16] that is, heating single crystals of **1** in water will gradually lead to formation of **3** and the single phase of isomer **2** will be obtained when the temperature is increased to 90 °C, as demonstrated by temperature-resolved PXRD patterns (see Figure 2b). Similarly, no structural transformation will occur via heating the single crystals of **1** in air in the temperature range 20−100 °C, though during which a clear color change from colorless to black is observed. Since the transformation from **2** to **1** can be regarded as a spontaneous process (at room temperature) compared with that from **1** to **2** (under hydrothermal conditions), complexes **1** and **2** can be ascribed to the thermodynamic and kinetic isomers that are closely related by interconversion with the same intermediate state **3** (see Figure 3). Although some nice examples for transformations between the thermodynamic and kinetic isomers have been recognized,[1b,17] observation of a mutual intermediate state during the conversion process as described in this work is unique.

Thermal Stability. The thermal stability of **1** and **2** was studied by thermogravimetric and differential scanning calorimetry (TG-DSC) experiments (see Figure S7, Supporting Information). The TG curve indicates that **1** is thermally stable to ca. 260 °C, and beyond this temperature, a sharp weight loss occurs. With that, the residual sample starts to gradually decompose with weight loss ending at ca. 690 °C. Upon further heating to 800 °C, no weight loss is observed and the final residue holds a weight of 41.2% of the total sample. Only one endothermic peak in 293 °C is observed in the DSC curve of **1**. For the TG curve of **2**, pyrolysis of the polymeric coordination framework is found upon heating to ca. 240 °C (one endothermic peak appearing at 278 °C in DSC) and then followed by another weight loss from ca. 400−540 °C with one exothermic peak observed at 438 °C in the DSC curve. Upon further heating to 800 °C, a slight weight loss occurs and the final residue has a weight of 42.0% of the total sample.

Luminescent Properties. The luminescence properties of complexes **1** and **2** were investigated at room temperature in the solid state. Both isomers display similar photoluminescence behaviors, that is, a single excitation peak at 372 nm that leads to the maximum emission at 424 nm for **1** or **2** and 425 nm for 2-bpt (see Figure S8, Supporting Information). This observation reveals that the emissions of **1** and **2** should exclusively originate from the intraligand transitions of 2-bpt. Moreover, visible decrement of the emission intensity of **1** and **2** in comparison with that of 2-bpt is observed, which may be attributed to the heavy atom effect of the Ag^{I} ion.[18]

CONCLUSIONS AND PERSPECTIVE

Two genuine supramolecular isomers of the coordination assembly by silver(I) nitrate and 2-bpt can be obtained under

hydrothermal conditions by properly selecting the organic acids as additive agents. In both morphs, the coordination geometry of Ag^{I} and the binding mode of 2-bpt are similar, and thus, the different orientations of the 2-bpt ligands are the crucial factor in dominating their superstructures. Remarkably, isomers **1** and **2** represent the thermodynamic and kinetic species, respectively, which show interisomerization behavior with observation of the same intermediate state. These results will provide new insights into the rational design and construction of supramolecular isomers of coordination assemblies and further develop possible supramolecular devices in the future.

■ ASSOCIATED CONTENT

Supporting Information. X-ray crystallographic files (CIF) for **1** and **2**, tables for selective bond parameters of **1** and **2** and some reaction parameters used to produce **1**, PXRD patterns for **1** and **2**, supplementary structural figures of **1** and **2**, solid-state CD spectra of **2** obtained in the presence of different additives, PXRD patterns for **1**−**3**, IR spectra for **1**−**3**, TG-DSC curves for **1**−**3**, and solid-state excitation/emission spectra of **1**, **2**, and 2-bpt. This material is available free of charge via the Internet at http://pubs.acs.org.

■ AUTHOR INFORMATION

Corresponding Author

*Phone/Fax: 86-22-23766556. E-mail: dumiao@public.tpt.tj.cn.

■ ACKNOWLEDGMENT

This work was financially supported by the National Natural Science Foundation of China (20971098 and 21031002), Program for New Century Excellent Talents in University (NCET-07-0613), Tianjin Natural Science Foundation (10JCZDJC21800), and Tianjin Normal University (No. 52X09004).

■ REFERENCES

(1) (a) Moulton, B.; Zaworotko, M. J. *Chem. Rev.* **2001**, *101*, 1629. (b) Zhang, J.-P.; Huang, X.-C.; Chen, X.-M. *Chem. Soc. Rev.* **2009**, *38*, 2385. (c) Cao, G.-J.; Lin, J.; Wang, J.-Y.; Zheng., S.-T.; Fang, W.-H.; Yang, G.-Y. *Dalton Trans.* **2010**, *39*, 8631. (d) Mahmoudkhani, A. H.; Shimizu, G. K. H. *Inorg. Chem.* **2007**, *46*, 1593. (e) Zheng, X.-D.; Lu, T.-B. *CrystEngComm* **2010**, *12*, 324. (f) Nangia, A. *Acc. Chem. Res.* **2008**, *41*, 595.

(2) (a) Zhang, J.-P.; Chen, X.-M. *Chem. Commun.* **2006**, 1689. (b) Jiang, J.-J.; Li, L.; Lan, M.-H.; Pan, M.; Eichhofer, A.; Fenske, D.; Su, C.-Y. *Chem.—Eur. J.* **2010**, *16*, 1841. (c) Kumar, D. K.; Das, A.; Dastidar, P. *Cryst. Growth Des.* **2007**, *7*, 2096. (d) Yang, L.-F.; Cao, M.-L.; Mo, H.-J.; Hao, H.-G.; Wu, J.-J.; Zhang, J.-P.; Ye, B.-H. *CrystEngComm* **2009**, *11*, 1114.

(3) (a) Fromm, K. M.; Doimeadios, J. L. S.; Robin, A. Y. *Chem. Commun.* **2005**, 4548. (b) Zheng, X.-D.; Jiang, L.; Feng, X.-L.; Lu, T.-B. *Inorg. Chem.* **2008**, *47*, 10858. (c) Jiang, L.; Lu, T.-B.; Feng, X.-L. *Inorg. Chem.* **2005**, *44*, 7056. (d) Jiang, L.; Feng, X.-L.; Su, C.-Y.; Chen, X.-M.; Lu, T.-B. *Inorg. Chem.* **2007**, *46*, 2637. (e) Zheng, X.-D.; Hua, Y.-L.; Xiong, R.-G.; Ge, J.-Z.; Lu, T.-B. *Cryst. Growth Des.* **2011**, *11*, 302.

(4) Li, C.-P.; Du, M. *Chem. Commun.* **2011**, *47*, 5958 and references cited therein.

(5) (a) Tong, M.-L.; Hu, S.; Wang, J.; Kitagawa, S.; Ng, S. W. *Cryst. Growth Des.* **2005**, *5*, 837. (b) Sun, D.-F.; Ke, Y. X.; Mattox, T. M.; Ooro, B. A.; Zhou, H.-C. *Chem. Commun.* **2005**, 5447. (c) Zhang, J.-P.; Lin, Y.-Y.; Huang, X.-C.; Chen, X.-M. *Cryst. Growth Des.* **2006**, *6*, 519. (d) Dai, F.-N.; He, H.-Y.; Sun, D.-F. *Inorg. Chem.* **2009**, *48*, 4613.

(6) (a) Zheng, B.; Dong, H.; Bai, J.-F.; Li, Y.-Z.; Li, S.-H.; Scheer, M. *J. Am. Chem. Soc.* **2008**, *130*, 7778. (b) Gütlich, P.; Hauser, A.; Spiering, H. *Angew. Chem., Int. Ed.* **1994**, *33*, 2024. (c) Ruiz-Molina, D.; Veciana, J.; Wurst, K.; Hendrickson, D. N.; Rovira, C. *Inorg. Chem.* **2000**, *39*, 617. (d) Ma, S.; Sun, D.; Ambrogio, M.; Fillinger, J. A.; Parkin, S.; Zhou, H.-C. *J. Am. Chem. Soc.* **2007**, *129*, 1858.

(7) (a) Su, Z.; Chen, M.; Okamura, T.; Chen, M.-S.; Chen, S.-S.; Sun, W.-Y. *Inorg. Chem.* **2011**, *50*, 985. (b) Sharma, M. K.; Bharadwaj, P. K. *Inorg. Chem.* **2011**, *50*, 1889. (c) Li, N.; Jiang, F.-L.; Chen, L.-A.; Li, X.-J.; Chen, Q.-H.; Hong, M.-C. *Chem. Commun.* **2011**, *47*, 2327. (d) Shiu, K. B.; Lee, H. C.; Lee, G. H. *Cryst. Growth Des.* **2010**, *10*, 2083. (e) Chatterjee, P. B.; Audhya, A.; Bhattacharya, S.; Abtab, S. M. T.; Bhattacharya, K.; Chaudhury, M. *J. Am. Chem. Soc.* **2010**, *132*, 15842.

(8) (a) Chen, X.-D.; Zhao, X.-H.; Chen, M.; Du, M. *Chem.—Eur. J.* **2009**, *15*, 12974. (b) Vittal, J. J. *Coord. Chem. Rev.* **2007**, *251*, 1781. (c) Chen, C.-L.; Goforth, A. M.; Smith, M. D.; Su, C.-Y.; zur Loye, H. C. *Angew. Chem., Int. Ed.* **2005**, *44*, 6673. (d) Das, D.; Engel, E.; Barbour, L. J. *Chem. Commun.* **2010**, *46*, 1676. (e) Zhang, Y. J.; Liu, T.; Kanegawa, S.; Sato, O. *J. Am. Chem. Soc.* **2009**, *131*, 7942.

(9) (a) Du, M.; Jiang, X.-J.; Zhao, X.-J. *Inorg. Chem.* **2007**, *46*, 3984 and references cited therein. (b) Du, M.; Zhang, Z.-H.; You, Y.-P.; Zhao, X.-J. *CrystEngComm* **2008**, *10*, 306.

(10) Bentiss, F.; Lagrenee, M. *J. Heterocycl. Chem.* **1999**, *36*, 1029.

(11) *SAINT Software Reference Manual*; Bruker AXS: Madison, WI, 1998.

(12) Sheldrick, G. M. *SHELXTL NT, Version 5.1, Program for Solution and Refinement of Crystal Structures*; University of Göttingen: Göttingen, Germany, 1997.

(13) Morris, R. E.; Bu, X. *Nat. Chem.* **2010**, *2*, 353.

(14) (a) Reichert, W. M.; Holbrey, J. D.; Vigour, K. B.; Morgan, T. D.; Broker, G. A.; Rogers, R. D. *Chem. Commun.* **2006**, 4767. (b) Morris, R. E. *Chem. Commun.* **2009**, 2990. (c) Cooper, E. R.; Andrews, C. D.; Wheatley, P. S.; Webb, P. B.; Wormald, P.; Morris, R. E. *Nature* **2004**, *430*, 1012.

(15) (a) Zhang, J.; Chen, S.-M.; Wu, T.; Feng, P.; Bu, X. *J. Am. Chem. Soc.* **2008**, *130*, 12882. (b) Zhang, J.; Chen, S.-M.; Nieto, R. A.; Wu, T.; Feng, P.; Bu, X. *Angew. Chem., Int. Ed.* **2010**, *49*, 1267. (c) Murali, C.; Shashidhar, M. S.; Gonnade, R. G.; Bhadbhade, M. M. *Chem.—Eur. J.* **2009**, *15*, 261. (d) Wu, L.-Z.; Wang, Q.-B.; Lu, J.-T.; Bian, Y.-Z.; Jiang, J.-Z.; Zhang, X.-M. *Langmuir* **2010**, *26*, 7489. (e) Guiry, K. P.; Coles, S. J.; Moynihan, H. A.; Lawrence, S. E. *Cryst. Growth Des.* **2008**, *8*, 3927.

(16) In this case, single crystals of **1** (ca. 100 mg) and water (10 mL) were sealed in a Teflon-lined stainless steel vessel (20 mL), heated at a fixed temperature for 12 h, and then cooled to room temperature for 1 day, affording the microcrystalline samples used for PXRD measurements. Notably, immersing the crystals of **1** in boiling water in a glass flask for 12 h will not lead to such a transformation.

(17) (a) Ratera, I.; Ruiz-Molina, D.; Vidal-Gancedo, J.; Novoa, J. J.; Wurst, K.; Letard, J.-F.; Rovira, C.; Veciana, J. *Chem.—Eur. J* **2004**, *10*, 603. (b) Näther, C.; Bhosekar, G.; Jess, I. *Inorg. Chem.* **2007**, *46*, 8079. (c) Zhang, J.-P.; Lin, Y.-Y.; Zhang, W.-X.; Chen, X.-M. *J. Am. Chem. Soc.* **2005**, *127*, 14162.

(18) Seward, C.; Chan, J.; Song, D.-T.; Wang, S.-N. *Inorg. Chem.* **2003**, *42*, 1112.